

# Investigation of Motion Illusions in Continuous Line Graphics on Geometric Forms through Eye-movement Analysis

Chih-Chao Chang,<sup>1</sup> Guang-Dah Chen,<sup>2</sup> and Chao-Ming Wang<sup>3\*</sup>

<sup>1</sup>Graduate School of Design, National Yunlin University of Science and Technology, Douliu 640301, Taiwan

<sup>2</sup>Department of Visual Communication Design, National Taiwan University of Arts, Banqiao, New Taipei City 22058, Taiwan

<sup>3</sup>Department of Digital Media Design, National Yunlin University of Science and Technology, Douliu 640301, Taiwan

(Received November 11, 2024; accepted April 15, 2025)

**Keywords:** visual perception, motion illusions, eye tracking, scan path, saccade amplitude

The study of motion illusions is a significant area of psychology and visual perception. Most motion illusions investigated so far are perceived from static objects. However, many objects exhibiting illusory motions are dynamic, which necessitates further investigation. In this study, the aim is to investigate the visual tracking of motion illusions generated by continuous line graphics on dynamically rotated geometric forms, using precise eye-movement data obtained through an eye-tracking system. Three types of motion illusion—apparent motion, induced motion, and motion aftereffect—are created by rotating seven different types of prism, including six polygonal shapes and one cylindrical shape. Properties of the eye-movement data, such as saccade amplitude, fixation count, and scan path, were analyzed by a psychophysical approach. The results reveal that the three types of motion illusion appear in a specific order as a prism is rotated from slow to fast. Among these illusions, apparent motion results in the largest average saccade amplitudes, and among the seven types of prism, the triangular prism induces the smallest average saccade amplitude. Additionally, the triangular prism is associated with the fewest number of fixations. These findings contribute to a deeper understanding of motion illusions, emphasizing their potential applications in eye-tracking research in daily contexts and offering valuable insights for future studies in visual perception.

## 1. Introduction

### 1.1 Background

In the field of visual perception, optical illusions (also known as visual illusions) are phenomena in which the visual system creates perceptions that may deviate from reality.<sup>(1,2)</sup> There are various types of optical illusion, one of which is *motion illusion* (also called *illusory motion*). In this category, stationary objects such as images, graphics, characters, or shapes appear to be in motion owing to cognitive effects resulting from interacting color contrasts,

---

\*Corresponding author: e-mail: [wangcm@yuntech.edu.tw](mailto:wangcm@yuntech.edu.tw)  
<https://doi.org/10.18494/SAM5467>

shape differences, and positional variations.<sup>(3,4)</sup> Researchers have identified the following three specific types of motion illusion.

1. *Apparent motion* is the perception of motion that occurs like an illusion when consecutive images or objects are displayed at a specific frame rate. A common example is the sequential motion seen in traditional films, which gives rise to the term “motion picture”.
2. *Induced motion* is another illusion created when a rapidly changing background contrasts with a stationary object, causing the object to appear as if it is moving. This effect is often observed in movies, such as when a plane flies against the sky, making it appear as though the plane itself is moving.
3. *Motion aftereffect* is a captivating illusion that occurs when a person watches a moving stimulus for an extended period and then shifts attention to a stationary object. The stationary object will then appear to move in the opposite direction of the original moving stimulus.

Figure 1 shows three examples of apparent-motion visual illusions apart from movies.

1. In Fig. 1(a), there is a zoetrope consisting of a cylinder with evenly spaced, vertical slits. Inside the cylinder, there is a strip of sequential images. By spinning the cylinder and peering through the holes from the outside, viewers can observe a continuous, looping motion sequence.<sup>(5)</sup>
2. Figure 1(b) shows two electronic commercial signs on the right, distinguished by their blue and red marquees. These signs employ the apparent-motion technique by flashing light dots on and off, creating the illusion of running advertisement texts.<sup>(3)</sup>
3. Figure 1(c) depicts a black-and-white picture. By fixating on the central circular vertical-bar pattern, one can observe that it seems to move relative to the horizontal-bar pattern in the surrounding area. This exemplifies the Ouchi apparent-motion illusion.<sup>(6)</sup>

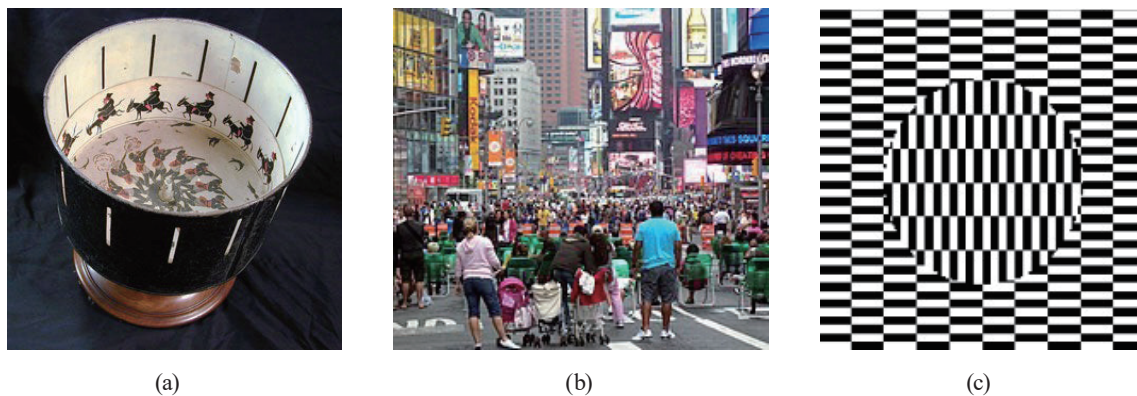


Fig. 1. (Color online) Three examples of objects exhibiting apparent-motion illusions. (a) A zoetrope, which is a cylindrical device adorned with evenly spaced vertical slits. As the cylinder spins, these slits reveal a captivating illusion of a continuous sequence of motion, like "a walking donkey ridden by a man".<sup>(5)</sup> (b) Red and blue electronic signs are seen on LED display boards to the right in the picture. Through the rapid flashing of light dots, these signs ingeniously create the illusion of a dynamic textual advertisement in motion.<sup>(3)</sup> (c) A mesmerizing graphic picture with a central circular vertical-bar pattern surrounded by a horizontal-bar pattern. When fixating upon the central pattern, the so-called Ouchi apparent-motion illusion occurs with the central pattern seemingly moving in relation to the surrounding pattern.<sup>(6)</sup>

Most motion illusions studied are perceived visually from *static* objects. Two such static objects, for example, are the commercial-sign LED display boards shown in Fig. 1(b) and the bar-pattern graphic picture shown in Fig. 1(c). These static objects themselves are *not really moving*; the motions perceived from them are merely *visual illusions*. In contrast, the objects explored in this study, which are observed to have illusory motions, were selected to be *dynamic*, i.e., the position and/or direction (or, more broadly, the displacement) of the object changes with time. An example of such objects is the barber pole,<sup>(7–9)</sup> which is traditionally placed outside a barber shop, like the one shown in Fig. 2(a). As illustrated in Fig. 2(b), the barber pole is a cylinder *dynamically* rotating around its vertical axis, with two mutually parallel diagonally striped colored bands printed on its surface. Although the cylinder rotates *horizontally* around its vertical axis, the stripes on its surface appear to move *upward* in the vertical direction, creating a visually illusory effect of the induced motion type. Another well-known example of the induced-motion illusion is the apparent relative movement of the scene outside a moving train. This movement is sensed visually by a passenger sitting inside the train, as illustrated in Fig. 3(a).<sup>(10)</sup>

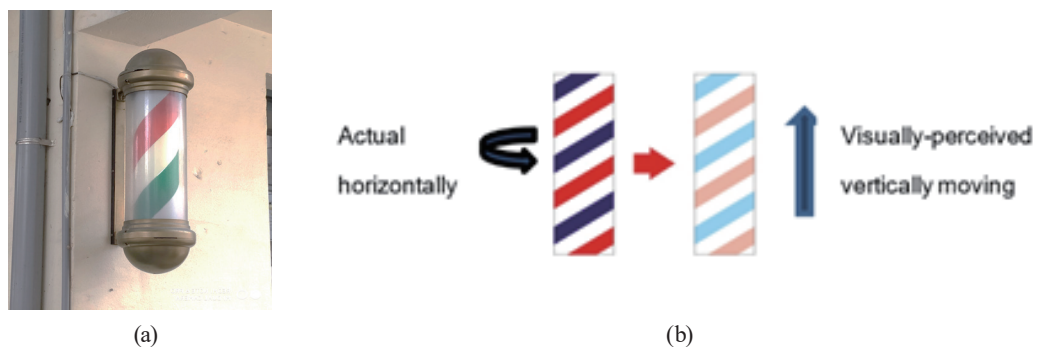


Fig. 2. (Color online) Barber-pole illusion created by a rotating diagonally striped sign. (a) A barber-pole sign.<sup>(9)</sup> (b) Actual and illusory motions of the barber pole.<sup>(7)</sup>

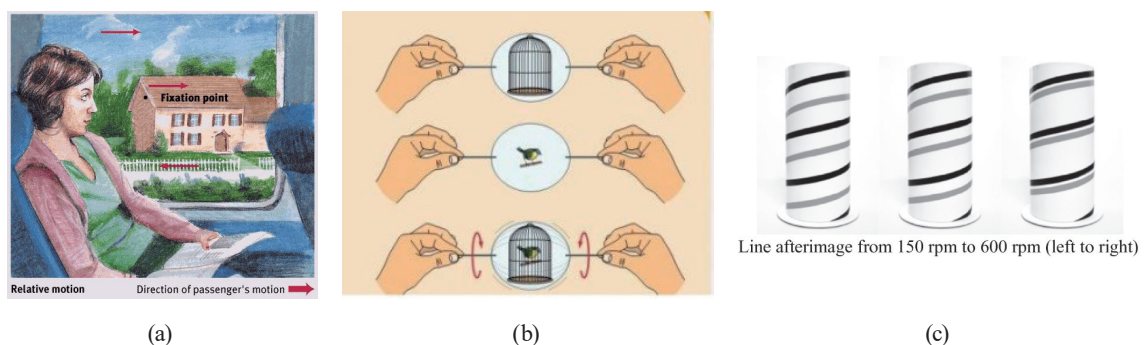


Fig. 3. (Color online) Induced-motion and motion-aftereffect illusions. (a) An induced-motion illusion (“The outside scene is moving backward!”) sensed visually by a passenger in a train.<sup>(10)</sup> (b) “Thaumatrope”, a classical example of the motion-aftereffect illusion (“The bird flies into the cage!”).<sup>(11)</sup> (c) Another example of the motion-aftereffect illusion where gray afterimages appear on a quickly rotated cylinder originally with only black spiral lines on the surface.<sup>(13)</sup>

As for the motion-aftereffect illusion, a classical example is the early animation toy, the “thaumatrope”, where the afterimage of a bird drawn on one side of a circular card appears to be in the cage drawn on the other side when the card is rotated quickly by twirling the strings connected to the two sides of the card,<sup>(11)</sup> as illustrated in Fig. 3(b). Note that the afterimage of the bird results from the persistence-of-vision (POV) function of the human eye.<sup>(12)</sup> A second example of the motion-aftereffect illusion is shown in Fig. 3(c), where the illusory afterimages—the gray lines—are produced by fast rotations of a cylinder (from 150 to 600 rpm) with black spiral lines on the surface.<sup>(13)</sup>

In summary, the main aim in this study is to conduct investigations on the human’s perception of illusory motions occurring on dynamic objects from various eye-movement perspectives. For simplicity, in this paper, illusory motions created by dynamic objects will be referred to as *dynamic illusory motion*, and the type of perception of such illusions will be termed *dynamic illusory motion perception*.

## 1.2 Research motivation

Recently, several studies on the perception of the rotational motions of dynamic objects have been conducted,<sup>(8,14,15)</sup> in which people’s reactions to dynamic illusory motions were observed through the correspondence between the physical stimulation (i.e., the rotational speed) and the psychological response (i.e., the intensity of the reaction). Positive research results have been obtained. However, more investigations regarding object types can still be carried out; specifically, the illusory motions (apparent motion, induced motion, and motion aftereffect) observed on dynamic *prism* objects may be studied further. Furthermore, an eye-tracking system with equipment like the EyeLink II headset<sup>(16)</sup> may be used to record precisely the participant’s eye movements during the observation of the involved dynamic object.

In more detail, studies of eye movements, which began in the 19th century and have made rapid progress in recent times,<sup>(8,17–20)</sup> included the analysis of the complicated human process of visual perception to provide valuable eye-movement data for related research studies. With the introduction of certain high-tech instruments for the more precise measurement of eye movements, the measurement of parameters such as *time instant* and *spatial condition* during data acquisition is becoming increasingly accurate, so that scholars in a growing number of fields have begun using eye-movement parameters as observation indicators in their studies and have conducted various eye-movement experiments to help further explore the relationship between human visual perceptions and eye-movement reactions. Nowadays, the observation indicators of eye movement are used extensively in research on topics such as attention,<sup>(21,22)</sup> reading,<sup>(23)</sup> pictorial perception,<sup>(24)</sup> visual search,<sup>(25)</sup> pattern recognition,<sup>(26)</sup> situational awareness,<sup>(27)</sup> and speeded saccadic and manual visuo-motor decisions.<sup>(28)</sup>

In short, the issue investigated in this study is the analysis of the visual processes involved in dynamic illusory motion perceptions by conducting experiments using the above-mentioned eye-tracking system and related techniques for recording the “pursuit movement” of the eyes, which is a basic form of eye movement. In the experiments, the eye-movement parameters such as time instant and spatial condition are measured precisely; that is, for the spatial-condition

parameter, the changes and distributions of the “scan paths” of the eyes, which are created from the perceptual reactions to the dynamic illusory motions when the participants viewed the dynamic object, were recorded, and for the time-instant parameter, the recorded data of “saccade amplitudes”, representing the eye-travel distances (related to the time of fixation shifts of the eyes) during the eye movements, are recorded as well.

### 1.3 Main indicators for observation of eye movements

Henderson and Hollingworth<sup>(25)</sup> stated that the complex human visual cognitive processes can be effectively understood in real time through the observation of eye movements. Therefore, to understand people’s visual data processing capability, analyses must be conducted using certain observation indicators of the eye movement. No fixed criteria exist for this purpose in current eye-movement studies; instead, different observation indicators should be used in various studies of different situations. As pointed out by Megaw and Richardson,<sup>(29)</sup> the analysis of observed eye-movement data may involve indicators such as saccade amplitude, fixation duration, fixation count, scan path, and pupil size.

1. *Saccade amplitude*: The displacement of a rapid movement of the eyes between two fixation points. For a person staring at a certain object, the average saccade amplitude can be used to represent the effective range of observation for each fixation point. Henderson and Hollingworth<sup>(25)</sup> stated that when people observe an image, the saccade amplitudes are significantly and directly related to the content of the image; in particular, when people watch a target with both images and text, a significant difference in saccade amplitudes will occur.
2. *Fixation duration*: The amount of time for which the center of the visual axis remains unchanged when people stare at an object, namely, the time from the end of one saccade movement of the eyes to the start of the next saccade movement (time unit: ms). Rayner<sup>(23)</sup> stated that, in visual searches, the average fixation duration per fixation point for a human is approximately 275 ms, whereas this duration increases to 330 ms in sense perception, and that the length of the fixation duration may be related to the richness of the image detail.
3. *Fixation count (number of fixations)*: The number of saccade movements, or equivalently, the number of fixation times, occurring when eyes are staring at an object. Buswell indicated in his study on image browsing behavior that when human eyes are staring at an image, the fixation points are not distributed randomly but tend to be regionally concentrated or scattered across various positions.<sup>(30,31)</sup> Therefore, the points focused on by people when viewing an image can be identified by analyzing the density of the fixation-point distribution with respect to the number of fixation points in each area of the image.
4. *Scan path (fixation-point sequence)*: The sequence of fixation points with saccades recorded according to a time sequence,<sup>(32–34)</sup> namely, an overall vision record consisting of “perception, movement, perception, ...” that can be observed in the eye movement. A scan path can specifically, intuitively, and comprehensively reflect the temporospatial features of the eye movement as well as the differences under various stimuli environments and experimental conditions.

5. *Pupil size*: A physiological indicator that can be used for measuring the sensitivity of the mental activity in terms of the visual mechanism.<sup>(35)</sup> It is known that a change in the pupil size can reflect the mental load: the greater the mental load, the larger the pupil size.<sup>(36–38)</sup>

#### 1.4 Research goals

As mentioned previously, most studies on eye movements were focused on illusions created by *static* objects; only a very few explored illusions coming from *dynamic* objects. That is, dynamic illusory motion perceptions have not been thoroughly studied. Static objects have no real states of motion; the illusory-motion effect induced by such objects depends mainly on the visual perception function. On the contrary, the dynamic illusory-motion effect involves time as a factor, i.e., it is generated by the displacement caused by the passage of time.

Given these factors and the conditions associated with dynamic illusory motion, what is the human visual process for perceiving a dynamic illusory motion induced by a dynamic object and what is the eye-movement mechanism involved? Are the visual movement direction and the eye-movement state in dynamic illusory-motion perception similar to those involved in the perception of illusions created by static objects? Are there changes occurring in the distribution of the resulting scan paths of the eyes? What distinct effects appear in human visual perceptions and eye movements? To answer these questions, in-depth explorations as conducted in this study are needed, and the following research tasks, which are taken as the goals of this study, should be accomplished:

1. study of the motion-illusion effects created by applying different rotation speeds to the prism-shaped objects;
2. exploration of the relationships existing between the perceptions of the three types of motion illusion and the saccade amplitudes and fixation counts in the eye-movement data measured during the illusion-perception process;
3. observation of the scan paths of the eye movements involved in the perceptual reactions to the three types of illusory motion incurred by different types of prism;
4. analysis of the difference between the two sexes in their visual reactions to the three types of motion illusion;
5. investigation of possible applications of the findings on the three motion-illusion perceptions; and
6. realization of more effective designs of dynamic geometric forms that satisfy human factors.

## 2. Literature Review

### 2.1 Effects of dynamic illusion phenomena

When people watch a dynamic object that creates motion illusions like the “barber-pole illusion”<sup>(14,39)</sup> mentioned previously, the visual effect perceived by human eyes is influenced by a number of factors, including the moving speed, viewing distance, and shape characteristics of the object. The illusory phenomena experienced by the eyes result from the relaxation and

contraction of the lens and the size of the retina, as well as the distance between the two eyes.<sup>(40)</sup> Specifically, when people observe the shape of a certain object at various distances, from a physical perspective, the smaller the distance is, the larger the object shape appears and the larger the viewing angle is, and vice versa. Thus, the viewing distance is related to the perceived size of the object. If the visually observed size of an object remains constant, the appropriate viewing distance can be determined using a set of formulas,<sup>(41)</sup> as illustrated in Fig. 4.

Studies on dynamic motion illusions caused by moving objects of certain shapes have been conducted by Chen.<sup>(1,39)</sup> In this study, the motion illusions caused by various prisms of polygonal and cylindrical shapes are investigated using the eye-movement data acquired by an eye-tracking system when the illusions are observed by participants.

## 2.2 Effects of dynamic illusion phenomena

Several studies have been conducted on the information of eye movements that occur during the visual perceptions of illusions, although some experiments have been conducted on the relationship between the generation of an illusion and the corresponding eye movements.

For example, two studies on the eye movements for observing the diagram of Müller-Lyer illusion (two horizontal line segments seem to have unequal lengths, but are actually the same), as shown in Fig. 5(a), were conducted by Fu and Sun<sup>(42)</sup> and Festinger *et al.*,<sup>(43)</sup> who assessed the eye movements during the visual process of viewing the Müller-Lyer illusion diagram and measured and compared the changes in the scan paths of the eyes. They concluded that the generation of illusions affects the pursuit movements of the eyes.

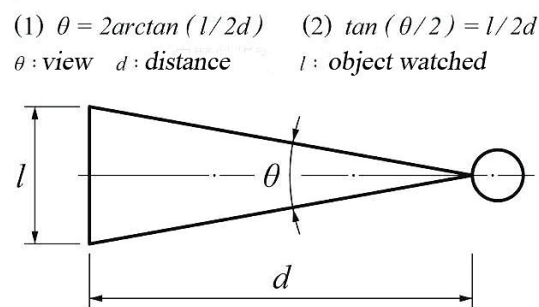


Fig. 4. Formula for computing the viewing angle of an object.<sup>(41)</sup>

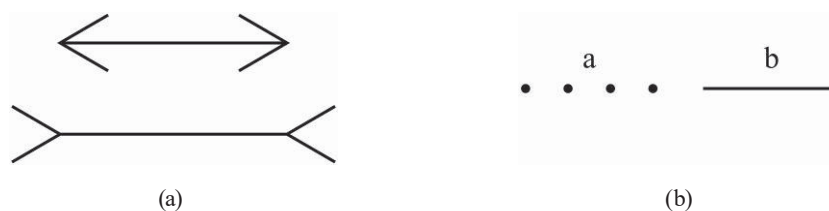


Fig. 5. Two optical illusion diagrams (drawn by the authors). (a) Müller-Lyer illusion diagram.<sup>(43)</sup> (b) Oppel-Kundt illusion diagram.<sup>(44)</sup>

Furthermore, Coren and Hoenig<sup>(44)</sup> investigated the eye movement occurring while viewing the diagram of the Oppel–Kundt illusion (the length of part a drawn with dots seems larger than that of part b drawn as a simple line segment, but actually is not), as shown in Fig. 5(b), and found the fact that a person with saccadic eye movements when viewing the diagram will feel a significant decrease in the percentage of perceiving the Oppel–Kundt illusion. Fu<sup>(45)</sup> studied the diagrams of the Hering–Wundt illusions (two straight and parallel lines presented in front of a radial background seem to be bowed outwards, but are actually not and the two blue vertical straight lines seem to be bowed inwards, but actually are not), as shown in Fig. 6(a), and Fu *et al.*<sup>(46)</sup> studied the Ebbinghaus illusion (the circle surrounded by small circles seems to be larger than the one surrounded by larger circles, but actually is not), as shown in Fig. 6(b), by measuring the scan-path changes of the eyes while observing the illusions, leading to the conclusion that the pursuit movements of the eyes are affected by diagrams that create optical illusions.

In the studies reviewed above, it was demonstrated that eye movements are significantly influenced by illusion diagrams, resulting in differences in the scan-path distributions. The respective findings regarding this aspect have validated relevant visual theories.<sup>(23,25,27)</sup>

### 2.3 Research method of psychophysics

“Psychophysics” is the science of studying the relationship between physical stimuli and psychological sensations. The method for examining the correspondence between mental quantities and physical quantities is the “psychophysical method,” which allows the relationship between the sensory system and the physical stimulation to be identified through the so-called “threshold” measurements.

Specifically, as stimulation gradually increases from low to high, it will eventually reach a value known as the “lower absolute threshold,” which produces a stimulus that the subject can feel. If the stimulation value continues to increase, it will reach another level, called the “upper absolute threshold,” beyond which the subject does not have the original sensory experience, but has a new one. The higher the absolute thresholds, the stronger the sensation experienced by the subject.<sup>(47)</sup>

Taking the experiments of this study as an example, the main purpose is to explore the correspondence between the rotation speed (rpm) of the polygonal prism and the reaction

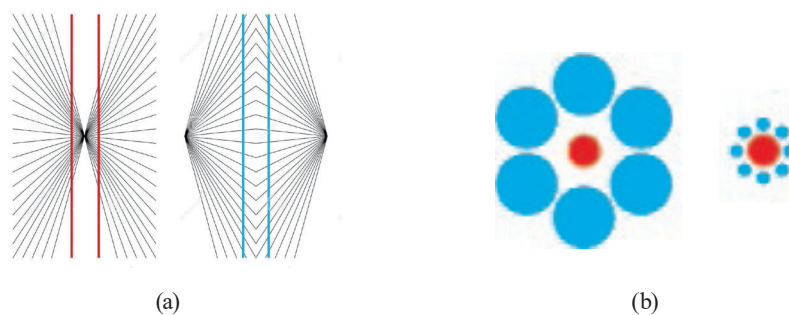


Fig. 6. (Color online) Three optical illusion diagrams (drawn by the authors). (a) Hering–Wundt illusion diagrams.<sup>(45)</sup> (b) Ebbinghaus illusion diagram.<sup>(46)</sup>

intensity of the dynamic motion-illusion perception of the participant. From the perspective of psychophysics, the speed (rpm) can be regarded as a kind of stimulation, and the reaction intensity of the subject to the dynamic motion illusion in the eye movement as a feeling. In this study, the regular relationship between the stimulation and the feeling is found by the psychophysical method.

In addition, there are three scientific methods for measuring the absolute thresholds used in psychophysics, namely, the method of constant stimuli, the method of limits, and the method of adjustment.<sup>(48)</sup> To allow the subject to directly respond to the stimulus size, the method of adjustment was used in this study. The advantage of this method is that the subject can actively participate in the experiment by adjusting the stimulus size to match a standard value, making it well suited to measuring absolute thresholds.<sup>(48)</sup>

## **2.4 Brief description of the research process of this study**

In this study, the research process includes primarily the following steps:

1. measure eye movements in response to the perceptual reactions to the dynamic illusory motions induced by dynamic objects;
2. observe the distributions and states of the scan paths of the perceptual reactions to the three types of illusory motion created by rotated prisms;
3. understand the visual moving direction and the eye-movement state associated with the three types of illusory motion; and
4. assess whether there are differences in the distributions and areas of the scan paths of the three types of illusory motion perception.

As mentioned previously, when a person observes an image, the more meaningful the content of the image, the larger the resulting saccades. In particular, eye saccades differ significantly when people look at a target object that has both images and text. Therefore, the observation index in the experiment conducted in this study will be based on saccade amplitude. For the purpose of in-depth analysis of the process of dynamic illusory motion perception, various eye-tracking experiments were carried out using the results of pursuing the eye movement, i.e., the pursuit motion results of the eyes. Another observation indicator, namely, the scan path of the eye movement, was used for the visual analysis of the perceptual reactions to the three types of dynamic illusory motion. This helped to understand how vision is affected by specific perceptions that cause changes in normal eye movements. Additionally, it enabled further exploration of the relationship between dynamic illusory motion perception and eye-movement reactions.

## **3. Research Method**

### **3.1 Experiments for creating the three types of illusory motion**

In this study, various phenomena and relationships between dynamic objects and dynamic illusory motion perceptions were investigated by the psychophysical method, the adjustment

method, and the scan-path measurement method of eye movements from the perspective of visual psychology. Additionally, the changes and distributions of the scan paths resulting from the perceptual reactions to the dynamic illusory motions during the participants' viewing process were recorded to understand their eye-movement reactions.

More specifically, the following three experiments were carried out in this study.

1. Experiment 1: Conducted during the perception of the illusion of *apparent motion* occurring on different types of prism to measure the eye-movement data
2. Experiment 2: Conducted during the perception of the illusion of *induced motion* occurring on different types of prism to measure the eye-movement data
3. Experiment 3: Conducted during the perception of the illusion of *motion aftereffect* occurring on different types of prism to measure the eye-movement data

### 3.2 Experimental system used in this study

The experimental system used in this study consists of the following four main parts.

1. Dynamic objects

The dynamic objects selected for this study are shown in Table 1:<sup>(8)</sup> six polygonal prisms with three to eight sides and a cylinder. Each of these prisms was rotated to create the three types

Table 1  
(Color online) Seven types of geometric prism used in this study.<sup>(8)</sup>

Prism type	Triangular prism	Quadrangular prism	Pentagonal prism
Prism label	P1	P2	P3
Top view			
Specimen			
Hexagonal prism	Heptagonal prism	Octahedral prism	Cylinder
P4	P5	P6	P7

of motion illusion for the participant to observe for the purpose of ascertaining whether different object types affect the resulting distributions of the scan paths of the perceptual reactions of the participants' eyes.

## 2. Object Rotation Mechanism

Before observation, each object was made to be *dynamic* by placing it on a turntable, securing it with a multifunctional disc holder, and rotating it with a series of speeds from slow to fast (in rpm) adjusted by a digital variable-frequency control system, as shown in Fig. 7(a).

## 3. Eye-tracking system

The rotated object is observed using an eye tracker, i.e., the EyeLink II headset,<sup>(16)</sup> part of an eye-tracking system that additionally includes a computer, as shown in Fig. 7(b), for processing the data collected through the headset, and a screen, as shown in Fig. 7(c), for displaying the data processing results.

## 4. System setup

The system setup, including a table and chair, for carrying out the experiments in this study is illustrated in Fig. 7(d). As shown, each participant is invited to sit on a chair in front of the object (a prism or a cylinder) to be observed at a distance of 100 cm from the object, with his/

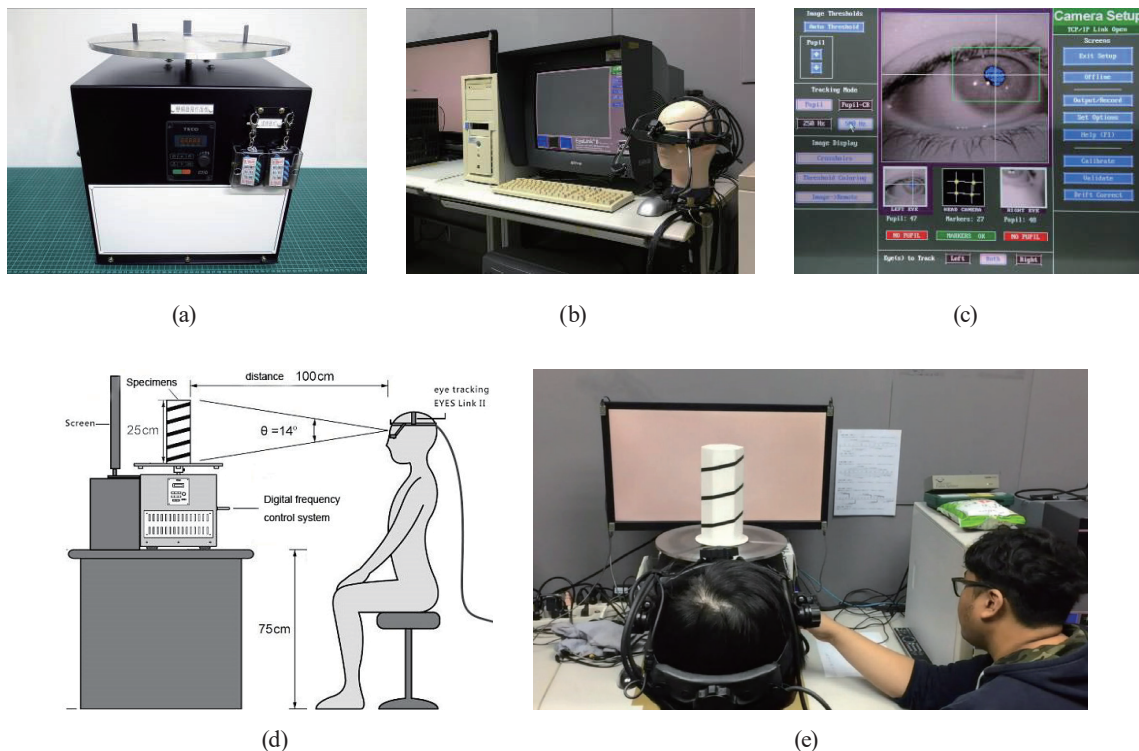


Fig. 7. (Color online) Experimental system used in this study. (a) A digital variable-frequency control system with a turntable on top for rotating the object. (b) An EyeLink II headset connected to a computer and a screen.<sup>(16)</sup> (c) Screen displaying the data processing results of the EyeLink II headset. (d) System setup for conducting the experiments where the participant sits in front of the system staring at the illusion created by a rotating prism. (e) Photograph of an experiment in which a rotating hexagonal prism is being viewed by a participant wearing an EyeLink II headset with an instructor sitting alongside.

her eyes staring at the rotating object with a view angle of about 14°. A real image of a participant using the experimental system is shown in Fig. 7(e).

### 3.3 Illusion changes created by rotating prisms

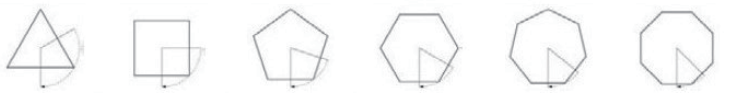
The basic concepts of the three types of motion illusion, i.e., apparent motion, induced motion, and motion aftereffect, were introduced previously with examples for each type being given. The concepts of these types of motion illusion are elaborated here.

#### 3.3.1 Rotating polygonal prisms to create the apparent-motion illusion

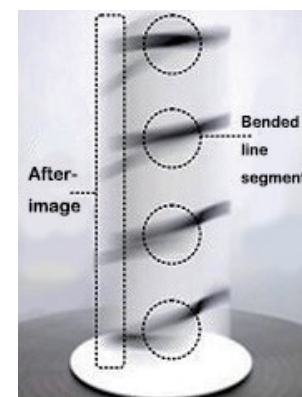
As mentioned previously, the effect of a traditional movie show is a phenomenon of the apparent-motion illusion. This illusion occurs when a sequence of discrete image frames is projected onto a screen at fixed time intervals, causing the images to appear visually continuous due to the POV capability of the human eyes. Specifically, the movie projector uses a shutter to block the film’s physical movement between two frames, ensuring that only the image grid is projected, which creates the POV-based apparent-motion illusion.<sup>(4,49)</sup> In this process, the time interval  $t_m$  for displaying the image frames should be adjusted to match the POV time  $t_v$  of the human eyes. It is known that  $t_v$  is about 0.1–0.4 s, and  $t_m$  for a 16 mm movie is typically 1/24 s.<sup>(49)</sup>

This principle of movie projection can be applied to each of the six polygonal prisms shown in Table 1 to generate apparent-motion illusions. The reason is that when a prism is rotated at a certain speed such that the sequence of its polygonal-shaped lateral sides appear consecutively at an appropriate time interval, the effect resembles movie projection, with the graphic lines on the prism surface appearing continuous like a rising spiral pattern. Here, the “rotation angle” between two neighboring lateral sides of the prism functions like a “shutter” of a movie projector, as shown in Fig. 8(a).<sup>(8)</sup> For this reason, the cylindrical prism (i.e., the cylinder) in Table 1 is not capable of creating an apparent-motion illusion, as no such “rotation angle” is formed on its smooth, continuous lateral surface.

Triangle column	Square column	Pentagon column	Hexagon column	Heptagon column	Octagon column
120°	90°	72°	60°	52°	45°



(a)



(b)

Fig. 8. Illustrations of rotation angles and afterimages.<sup>(8)</sup> (a) “Rotation angles” of polygonal prisms (columns). (Note: the smooth surface of the cylinder has no rotation angle.) (b) Afterimages occurring when a polygonal prism is rotated very fast.

### 3.3.2 Rotating polygonal prisms to incur the induced-motion illusion

As mentioned previously, by moving a fast-changing background around a fixed object, an induced-motion illusion will appear with the illusory effect of the object moving against the background, as seen in the film of a traditional movie including a plane flying in the sky.

Alternatively, as mentioned by Chen and Chang,<sup>(50)</sup> an induced-motion effect can be created by rotating a polygonal or cylindrical prism, as shown in Table 1, at a sufficiently high speed (faster than the rotation speed mentioned previously for creating the apparent-motion effect), causing the white areas on the lateral sides, much larger than the spiral lines, to become “assimilated” into a single connected white region that appears stationary, leaving only the spiral pattern spinning upward.

### 3.3.3 Rotating polygonal prisms to incur the motion-aftereffect illusion

As mentioned previously, when a stationary object is viewed right after observing a moving stimulus for an extended period, the stationary object appears to move visually, creating a motion-aftereffect illusion.

Alternatively, as pointed out by Chen and Chang<sup>(50)</sup> again, when a polygonal or cylindrical prism is rotated very fast, with all the white lateral parts of the object becoming assimilated to form a large region, as mentioned above, all the spiral line segments will appear simultaneously on the rotating object’s surface as an afterimage, creating an illusion similar to the motion-aftereffect effect [called *motion afterimage* in Chen and Chang<sup>(50)</sup>] owing to the POV function of the human eyes, as shown in Fig. 8(b).

### 3.3.4 A concluding remark.

By integrating the three phenomena described previously, the following conclusion can be drawn.

*As the rotation speed of each of the polygonal or cylindrical prisms is increased from slow to very fast, the three types of motion illusion can be sensed visually by the human eyes in the following order:*

*apparent motion → induced motion → motion aftereffect.*

## 3.4 Average rotation speed ranges to create the three types of motion illusion

Overall, 20 persons (10 women and 10 men) were invited to participate in the experiment conducted in this study. They all passed the color-blindness test. During the experiment (described in detail later), the main task involved the participant observing each polygonal or cylindrical prism to experience visually the three types of motion illusion. The minimum and maximum rotation speeds for each of the three types of illusion motion for each of seven types of prism were recorded. From the resulting data, for each of the seven types of prism, the

absolute minimum speed and the absolute maximum speed, called the *absolute lower and upper thresholds*, respectively, were identified and are listed in Table 2. Note that the total range of speeds for all the prisms is from 70 to 330 rpm, as can be seen from the table [from the smallest absolute lower threshold (70 rpm) of P1 to the largest absolute upper threshold (330 rpm) of P7]. In practice, to allow participants time to familiarize themselves with each rotated prism, the rotation started at 35 rpm in the experimental process.

Accordingly, the ranges defined by the absolute lower and upper thresholds of the rotation speeds of, for example, the triangular prism to create the three types of illusion are (70, 90), (80, 180), and (170, 210) in the unit of rpm, respectively. That is, when the rotation speed is between 70 and 90 rpm, an apparent-motion illusion can be observed on the triangular prism, when the speed is faster, from 80 to 180 rpm, an induced-motion illusion is visually perceived, and when the speed is from 170 to 210 rpm, a motion-aftereffect illusion appears. Note that the three speed ranges have two overlapping parts, namely, 80 to 90 and 170 to 180 rpm. This overlap is due to the possible ambiguity for the participants to determine the type of motion illusion that they observed when the object was rotated at speeds falling within these overlapping ranges. Similar overlapping ranges also exist for other types of prism.

### 3.5 Eye-tracking system used in the experiment

In this study, the eye-tracking equipment EyeLink II headset, manufactured by SR Research Company<sup>(16)</sup> and shown in Figs. 7(b) and 7(c), was used for acquiring and processing eye-movement data automatically while the participant stared at the rotating prism during the experimental process. Although a few studies on the topic of dynamic illusory-motion analysis exist, this type of equipment was not used in those studies. A major advantage of using such equipment is its usefulness for realizing the fast and precise acquisition of eye-movement data.

More specifically, the EyeLink II headset is equipped with two miniature cameras on the left and right sides of the hood to record the position and pupil size of each eye, respectively,

Table 2  
Absolute lower and upper thresholds of rotation speeds (rpm) of the seven types of prism that incur the three types of motion illusion.

Absolute rotation-speed thresholds for creating apparent-motion illusions							
Prism label	P1	P2	P3	P4	P5	P6	P7*
(a) absolute lower threshold	70	80	70	50	40	35	—
(b) absolute upper threshold	90	60	50	65	60	50	—
Absolute rotation-speed thresholds for creating induced-motion illusions							
Prism label	P1	P2	P3	P4	P5	P6	P7
(a) absolute lower threshold	80	75	70	60	60	50	40
(b) absolute upper threshold	180	200	230	240	260	275	280
Absolute rotation-speed thresholds for creating motion-aftereffect illusions							
Prism label	P1	P2	P3	P4	P5	P6	P7
(a) absolute lower threshold	170	200	220	240	250	270	290
(b) absolute upper threshold	210	240	260	280	290	310	330

\*Cylinder P7 cannot be used to create apparent-motion illusions.

allowing monocular or binocular eye tracking based mainly on pupil movement and iris reflex to calculate the eye movement. Furthermore, the front of the hood is equipped with a miniature camera, and four infrared sensors are affixed on the associated display screen to calibrate the position of the user's head (expressed as 3D coordinates). Finally, associated with the headset are software packages on the computer for quickly converting the raw eye-movement data into statistical data and visualization diagrams, including saccade altitudes, fixation-point maps, and scan-path diagrams.

### 3.6 Learning prior to the experimental process

Before the experiment started, a learning procedure was conducted, in which an accompanying instructor taught the participant how to use the turntable to rotate the test prism and observe the dynamic illusory-motion phenomena during its rotation. Then, the participant was allowed to practice the procedure three times to become familiar with the judgements of the three types of motion illusion.

Subsequently, the instructor helped the participant put on the EyeLink II headset and start the fixation-position calibration process of the equipment, which includes two stages, namely, a 9-point calibration stage and a 9-point validation stage. Consequently, the eye-tracking equipment, with the help of the computer, can be utilized to calculate the precise position of a fixation point of the participant on the dynamic object (i.e., a polygonal or cylindrical prism rotating on the turntable) corresponding to the eye-movement angle of the participant using the calibration and verification results.

Specifically, the two stages of 9-point calibration and 9-point validation were carried out by performing the following steps.

1. A gaze dot for the participant to stare at appears randomly at one of nine predefined calibration positions: the center, top, bottom, left, right, upper right, lower right, upper left, and lower left on the test prism.
2. The participant is asked to stare at the dot steadily for 5 to 10 s and then press the space bar on the computer keyboard to confirm the gaze position.
3. The gaze dot immediately disappears, and Steps (1) through (3) are repeated, until the 9 calibration positions have all been processed.

### 3.7 Experimental process

In the experimental process, after each of the 20 invited participants has sat in front of the experimental system, as shown in Fig. 7(d) or 7(e), the following algorithm is carried out by the experimental system itself, or by the participant or the accompanying instructor who follows the instructions issued by the system.

**Algorithm: Acquisition of visual reaction data from perceptions of motion illusions.**

**Steps.**

- (1) Instruct the participant to pick up a test prism in the order of P1 through P7 as shown in Table 1 and place it on the turntable.

- (2) Start the digital variable-frequency control system to rotate the prism.
- (3) Gradually increase the rotation speed of the turntable from 35 to 330 rpm.
- (4) Instruct the participant to stare at the rotated prism continuously for 5 to 10 s and press the space bar on the computer keyboard to confirm the visual sensing of a type of motion illusion.
- (5) Record the participant's eye-movement data.
- (6) Compute the saccade amplitudes, the number of fixation times, and the scan paths using the data obtained in the last step.
- (7) Repeat Steps (3) through (6) until all three types of motion illusion are observed;
- (8) Repeat all the steps from (1) through (7) until data from all seven types of prism are acquired.

The experiment ended when all the 20 invited participants had completed the above experimental process. Afterwards, the collected eye-movement data from all the participants were combined and analyzed statistically. The results are described below.

## **4. Results**

### **4.1 Analyzed items of experimental data**

The following data items were recorded during the rotations of the objects using the digital variable-frequency control system, or extracted from the eye-movement data recorded by the eye-tracking system (i.e., the EyeLink II headset and the associated computer):

1. the absolute lower and upper thresholds of the object rotation speeds at which the three types of motion illusion, that is, apparent motion, induced motion, and motion aftereffect, were created, as listed in Table 2;
2. the average saccade amplitudes of the participants when staring at each of the seven types of prism to observe each of the three types of illusory motion, as shown in Figs. 9, 11, and 13;
3. the average numbers of fixation times of the participants when staring at each of the seven types of prism to observe each of the three types of illusory motion, as shown in Figs. 10, 12, and 14;
4. the average saccade amplitudes of the male and female participants extracted from the data of 2 above, as shown in Tables 3–5;
5. the distributions of the scan paths of a participant's perceptual reactions to the three types of illusory-motion perception created by the triangular prism, as shown in Figs. 15(a)–15(c) (shown as an example to illustrate scan-path diagrams).

### **4.2 Results of apparent-motion perception**

The experimental results regarding the participants' perceptions of the apparent-motion illusion and the related eye-movement data are shown in Figs. 9 and 10 and Table 3, from which the following facts or findings can be drawn.

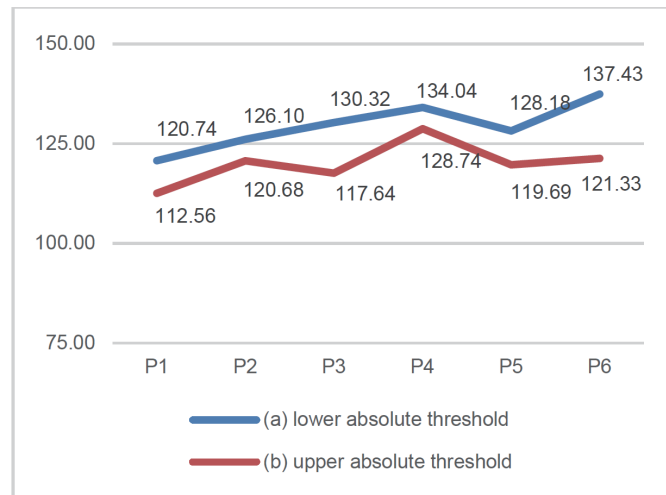


Fig. 9. (Color online) Average saccade amplitudes in observing the apparent-motion illusion created by the six types of polygonal prism (unit: pixel).

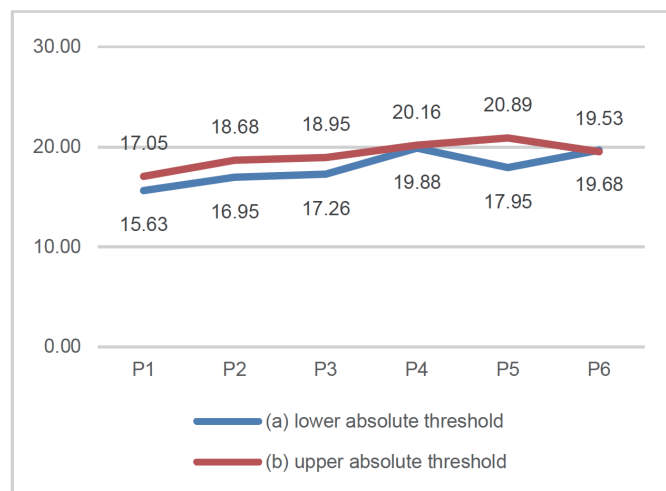


Fig. 10. (Color online) Average fixation counts in observing the apparent-motion illusion created by the six types of polygonal prism (unit: time).

#### 4.2.1 About the saccade amplitudes

(1) From Fig. 9, it can be seen that increasing the number of lateral sides of a polygonal prism progressively leads to the following two facts.

(a) The minimum average saccade amplitude of all the participants (referred to as the lower absolute threshold of the saccade amplitude) increases progressively in general.

(b) The maximum average saccade amplitude of all the participants (referred to as the upper absolute threshold of the saccade amplitude) also progressively increases in general.

These findings suggest that *the more lateral sides a polygonal prism has, the larger are the saccade amplitudes observed in the eye movement data for apparent-motion illusion perceptions, and vice versa.*

Table 3

Results of independent sample *t*-test applied to the average saccade amplitudes of the two sexes for the six types of polygonal prism for the apparent-motion illusion (M: male; F: female; S. D.: standard deviation).

Prism label**	Gender	<i>n</i>	Mean	S. D.	<i>p</i>
P1(a)	M	10	118.07	57.59	0.67
	F	10	107.05	57.09	
P1(b)	M	10	123.17	82.10	0.89
	F	10	118.30	73.64	
P2(a)	M	10	126.26	63.74	0.70
	F	10	115.10	62.91	
P2(b)	M	10	130.18	92.50	0.83
	F	10	122.02	73.85	
P3(a)	M	10	108.90	59.88	0.57
	F	10	126.37	73.32	
P3(b)	M	10	121.82	76.03	0.59
	F	10	138.82	59.59	
P4(a)	M	10	99.45	67.64	0.06
	F	10	158.03	64.27	
P4(b)	M	10	135.05	58.18	0.94
	F	10	133.03	61.66	
P5(a)	M	10	126.10	60.14	0.59
	F	10	113.28	42.41	
P5(b)	M	10	141.63	50.01	0.19
	F	10	114.73	37.35	
P6(a)	M	10	129.77	64.03	0.50
	F	10	112.89	42.86	
P6(b)	M	10	139.84	66.20	0.87
	F	10	135.01	59.26	

\*\* $P_i(a)$  and  $P_i(b)$  with  $i = 1, 2, \dots, 6$  mean the absolute lower and upper thresholds of saccade amplitudes for the polygonal prism labelled  $P_i$ .

(Note: cylinder P7 creates no apparent-motion illusion because no “rotation angle” is formed on it to yield a shutter effect when the cylinder is rotated, as mentioned previously.)

(2) From Fig. 9 again, the following two facts can be understood.

(a) The average saccade amplitude of the lower absolute threshold for a triangular prism was 120.74 pixels, which was the smallest among those of all the polygonal prisms.

(b) The average saccade amplitude of the upper absolute threshold for a triangular prism was 112.56 pixels, which was also the smallest among those of all the polygonal prisms.

Together with the finding of (1) above, these results indicate the following two observations about the perception of the apparent-motion illusion.

(a) The lower the saccade amplitude, the more centralized the fixation points.

(b) The triangular prism was stared at with the smallest saccade amplitude.

#### 4.2.2 About the fixation count

(1) By a reasoning similar to that above, in Fig. 10, it can be seen that progressively increasing the number of a polygonal prism’s lateral sides leads to the following two facts.

(a) The minimum average number of fixation times (called the lower absolute threshold of the fixation count) will increase progressively in general.

- (b) The maximum average number of fixation times (called the upper absolute threshold of the fixation count) will also increase progressively in general.

These findings suggest that *the more lateral sides a polygonal prism has, the larger is the fixation count in the eye movement data for the perception of the apparent-motion illusion, and vice versa.*

- (2) From Fig. 10 again, the following two facts can be observed.

- (a) The average fixation count at the lower absolute threshold of a triangular prism is 15.63, which was the smallest among those of all the polygonal prisms.
- (b) The average fixation count at the upper absolute threshold of a triangular prism was 17.05, which was the smallest among those of all the polygonal prisms.

These findings lead to the following two facts about the perception of the apparent-motion illusion.

- (a) The lower the saccade amplitude, the smaller the fixation count.
- (b) The triangular prism is stared at for the smallest number of fixation times.

#### 4.2.3 Differences between the two sexes in apparent-motion illusion perceptions

An independent sample  $t$ -test<sup>(51)</sup> was conducted on the saccade amplitudes in the eye-movement data of the two sexes (including the 10 male and 10 female participants) acquired when they were observing the apparent-motion illusion. The results are shown in Table 3, which includes the means and standard deviations of the data for each of the six polygonal prisms, and the  $p$ -values of the  $t$ -test results. In addition, in the table,  $P_i(a)$  and  $P_i(b)$  with  $i = 1, 2, \dots, 6$  refer, respectively, to the absolute lower and upper thresholds of saccade amplitudes for the polygonal prism labelled  $P_i$ .

It is known that if the  $p$ -value is smaller than 0.05, there is an obvious difference between the tested data acquired by the participating men and women. Accordingly, as shown in the last column of Table 3, for each of the six types of polygonal prism, the  $p$ -values are all larger than 0.05, showing that no significant difference exists between male and female participants in the aspect of reaction (shown by the lower and upper absolute thresholds of saccade amplitudes of eye-movement data) to the apparent-motion illusions incurred by the six types of polygonal prism.

### 4.3 Results of induced-motion perception

The experimental results of the induced-motion perception and the related eye-movement data are shown in Figs. 11 and 12 and Table 4, from which the following facts or findings can be drawn.

#### 4.3.1 About the saccade amplitudes

- (1) From Fig. 11, it can be seen that increasing the number of lateral sides of a polygonal prism progressively leads to the following two findings.

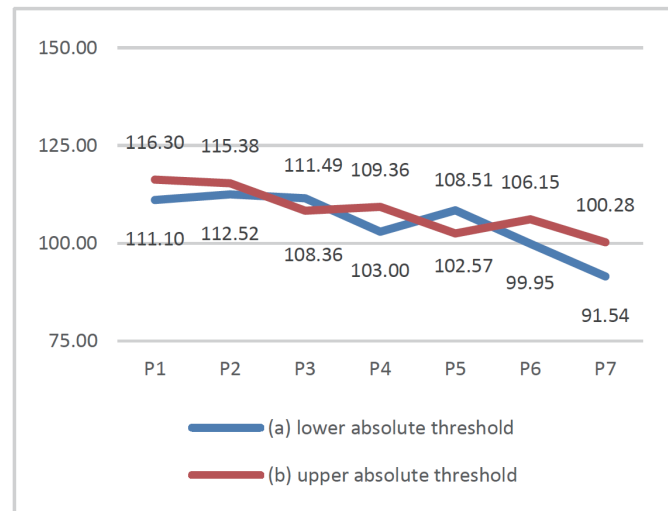


Fig. 11. (Color online) Average saccade amplitudes incurred in observing induced-motion illusions created by the seven types of prism (unit: pixel).

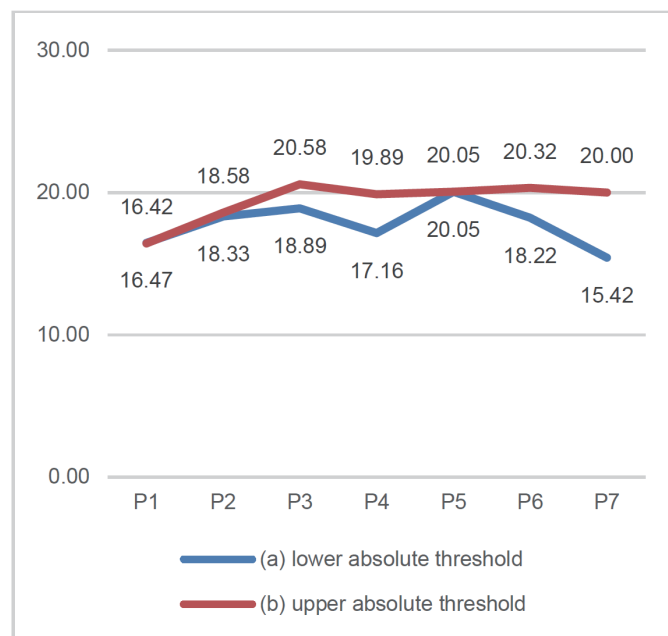


Fig. 12. (Color online) Average fixation counts incurred in the induced-motion illusion created by the seven types of prism (unit: time).

- (a) The lower absolute threshold of the saccade amplitude decreases progressively in general.
- (b) The upper absolute threshold of the saccade amplitude also decreases progressively in general.

Table 4

Results of independent sample  $t$ -test applied to the average saccade amplitudes of the two sexes for the seven types of prism for the induced-motion illusion (M: male; F: female).

Prism label <sup>***</sup>	Gender	$n$	Mean	S. D.	$p$
P1(a)	M	10	121.55	42.87	0.27
	F	10	111.05	40.76	
P1(b)	M	10	110.47	61.90	0.96
	F	10	111.72	55.08	
P2(a)	M	10	117.96	66.49	0.85
	F	10	112.51	52.39	
P2(b)	M	10	111.26	68.58	0.93
	F	10	113.79	50.18	
P3(a)	M	10	121.63	65.55	0.31
	F	10	95.09	45.61	
P3(b)	M	10	111.99	63.93	0.97
	F	10	110.99	39.89	
P4(a)	M	10	124.76	83.54	0.34
	F	10	93.96	52.82	
P4(b)	M	10	110.33	61.15	0.52
	F	10	95.67	34.36	
P5(a)	M	10	112.62	63.21	0.42
	F	10	92.52	44.80	
P5(b)	M	10	138.22	75.14	0.05
	F	10	78.80	48.91	
P6(a)	M	10	112.10	53.12	0.59
	F	10	100.19	42.97	
P6(b)	M	10	109.35	68.66	0.51
	F	10	90.56	54.51	
P7(a)	M	10	112.50	57.10	0.29
	F	10	88.06	41.00	
P7(b)	M	10	95.85	51.06	0.70
	F	10	87.23	47.29	

<sup>\*\*\*</sup>P<sub>*i*</sub>(a) and P<sub>*i*</sub>(b) with  $i = 1, 2, \dots, 7$  mean the absolute lower and upper thresholds of saccade amplitudes for the prism labelled P<sub>*i*</sub>.

These findings suggest that *the more lateral sides a prism has, the smaller are the saccade amplitudes found in the eye-movement data for induced-motion illusion perceptions, and vice versa.*

(Note: the above finding is also true for cylinder P7, which can be considered as a polygonal prism with an infinite number of lateral sides).

(2) From Fig. 11 again, the following two facts can be understood.

(a) The average saccade amplitude at the lower absolute threshold of a cylindrical prism was 91.54 pixels, which was the smallest among those of all the prisms.

(b) The average saccade amplitude at the upper absolute threshold of a cylindrical prism was 100.28 pixels, which was also the smallest among those of all the prisms.

Together with the findings of (1) above, these results indicate the following two facts about the perception of the induced-motion illusion.

(a) The smaller the saccade amplitude, the more centralized the fixation points.

(b) The cylindrical prism was stared at with the largest saccade amplitude.

### 4.3.2 About the fixation count

- (1) Unlike the case of the apparent-motion illusion, the trends of the fixation count are not so obvious when the number of lateral sides of the prism increases. Specifically, as the number of lateral sides of the prism increases, the following two facts can be seen from Fig. 12.
- (a) The lower absolute threshold of the fixation count increases for the first three types of prism and remains roughly the same for the remaining four types of prism.
  - (b) The upper absolute threshold of the fixation count has no fixed increasing or decreasing trend.
- (2) From Fig. 12 again, the following two facts can also be understood.
- (a) The average fixation count at the lower absolute threshold of a triangular prism was 16.47, which was the smallest among those of all the prisms.
  - (b) The average fixation count at the upper absolute threshold of a triangular prism was 16.42, which was also the smallest among those of all the prisms.

Together with the findings of (1) above, these results indicate the following two facts about the visual sensing of the induced-motion illusion.

- (a) The smaller the saccade amplitude, the smaller the fixation count.
- (b) The triangular prism is stared at for the smallest number of fixation times.

### 4.3.3 Differences between the two sexes in induced-motion illusion perceptions

Similarly to the case of apparent-motion illusion perception, an independent sample  $t$ -test<sup>(51)</sup> was conducted on the saccade amplitudes in the eye-movement data of the two sexes acquired when they were observing the induced-motion illusion. The results are shown in Table 4. As indicated in the last column of the table, for each of the seven types of prism, the  $p$ -values are all larger than 0.05, showing that no significant difference exists between the male and female participants in their reactions to the induced-motion illusions incurred by the seven types of prism.

## 4.4 Results of motion-aftereffect perception

The experimental results of the motion-aftereffect perception and the related eye-movement data are shown in Figs. 13 and 14 and Table 5, from which the following facts or findings can be drawn.

### 4.4.1 About the saccade amplitudes

- (1) From Fig. 13, it can be seen that increasing the number of lateral sides of a polygonal prism leads to the following fact:
- the lower absolute threshold of the saccade amplitude increases progressively in general.*
- This finding suggests that *the more lateral sides a polygonal prism has, the larger are the saccade amplitudes in the eye-movement data for motion-aftereffect illusion perception, and vice versa.*

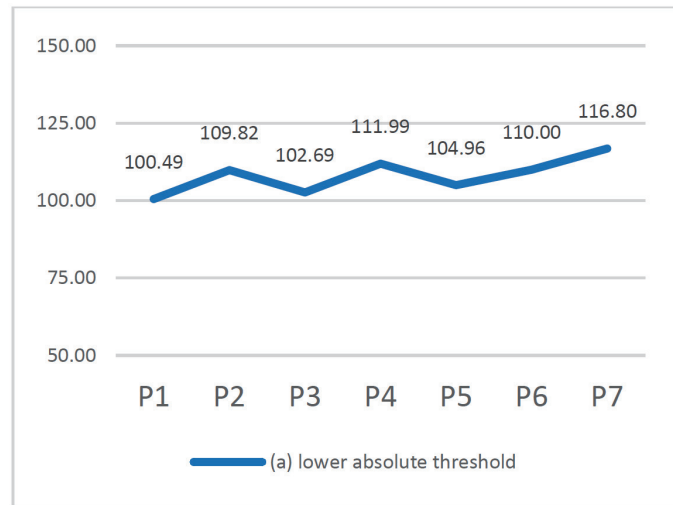


Fig. 13. (Color online) Lower absolute thresholds of the average saccade amplitudes incurred in observing the motion-afereffect illusion created by the seven prism types (unit: pixel).

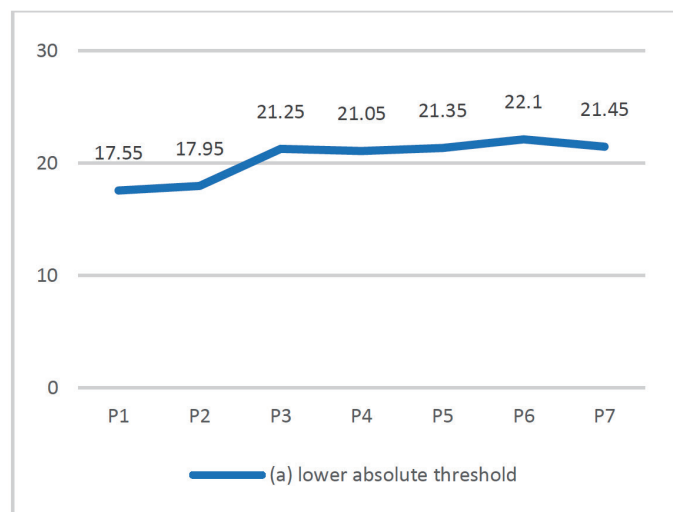


Fig. 14. (Color online) Lower absolute thresholds of the average fixation count incurred in observing the motion-afereffect illusion created by the seven prism types (unit: time).

(Note: after the rotation speed is increased to be larger than the absolute lower threshold, the illusion phenomenon will continue *endlessly* while the rotation speed continues to increase without an upper limit; therefore, there is no saccade-amplitude record of the absolute upper threshold in Fig. 13.)

#### 4.4.2 About the fixation count

(1) As the number of lateral sides of the prism increases, the following fact can be seen from Fig. 14:

Table 5

Results of independent sample  $t$ -test applied to the average saccade amplitudes of the two sexes for the seven types of prism for motion aftereffect (M: male; F: female).

Prism label***	Gender	$n$	Mean	S. D.	$p$
P1(a)	M	10	110.47	61.90	0.39
	F	10	111.72	55.08	
P2(a)	M	10	111.26	68.58	0.34
	F	10	113.79	50.18	
P3(a)	M	10	111.99	63.93	0.14
	F	10	110.99	39.89	
P4(a)	M	10	110.33	61.15	0.61
	F	10	95.67	34.36	
P5(a)	M	10	138.22	75.14	0.27
	F	10	78.80	48.91	
P6(a)	M	10	109.35	68.66	0.46
	F	10	90.56	54.51	
P7(a)	M	10	95.85	51.06	0.13
	F	10	87.23	47.29	

\*\*\*  $P_i(a)$  with  $i = 1, 2, \dots, 7$  means the absolute lower thresholds of saccade amplitudes for the prism labelled  $P_i$ .

*the lower absolute threshold of the fixation count increases for the first three types of prism and remains roughly the same for the remaining four types of prism.*

(2) From Fig. 14 again, the following fact can be understood:

*the average fixation count at the lower absolute threshold of a triangular prism was 17.55, which was the smallest among those of all the prisms.*

Together with the finding of (1) above, this result indicates the following two facts about the perception of the induced-motion illusion.

- (a) The smaller the saccade amplitude, the smaller the fixation count.
- (b) The triangular prism is stared at for the smallest number of fixation times.

#### 4.4.3 Differences between the two sexes in motion-aftereffect illusion perception

Similarly to the case of apparent-motion illusion perception, an independent sample  $t$ -test<sup>(51)</sup> was conducted on the saccade amplitudes in the eye-movement data of the two sexes acquired when they were observing the motion-aftereffect illusion. The results are shown in Table 5. As indicated in the last column of the table, for each of the seven types of prism, the  $p$ -values are all larger than 0.05, meaning that no significant difference exists between male and female participants in their reactions to motion-aftereffect perception for the seven types of prism.

#### 4.5 Examples of scan-path distributions in illusory-motion perception

As an example of the distributions of saccade amplitudes, the scan paths occurring during a participant's perceptions of the three types of motion illusion incurred by the triangular prism are shown in Figs. 15(a)–15(c).

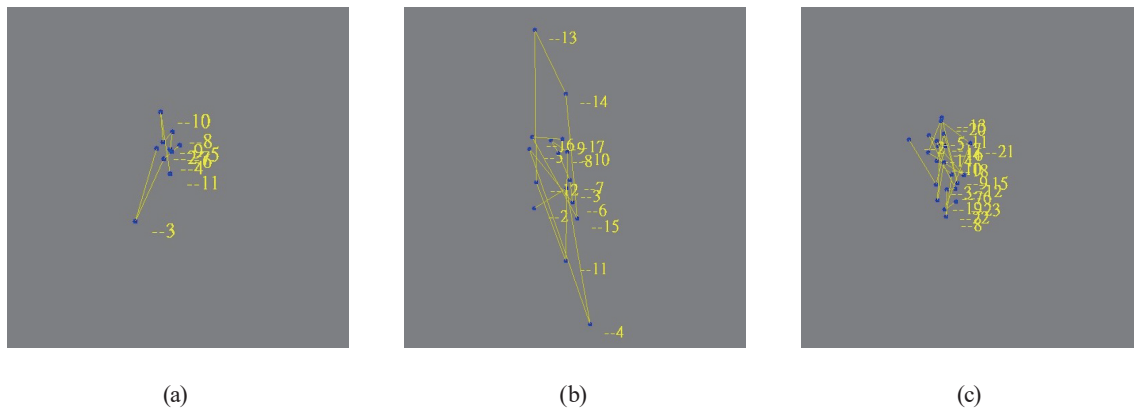


Fig. 15. (Color online) Diagrams of the scan paths in a participant's eye-movement data of the three motion illusions incurred by a triangular prism. (a) Shorter and centralized scan paths created by the apparent-motion illusion. (b) Upward moving and dispersed scan paths created by the induced-motion illusion. (c) Centralized scan paths created by the motion-afereffect illusion.

From the figures, it can be seen that the scan paths for the apparent-motion illusion are shorter and more centralized, as shown in Fig. 15(a); those for the induced-motion illusion are dispersed over a larger area and move up and down, as shown in Fig. 15(b); and finally, those for the motion-afereffect illusion are also centralized, as shown in Fig. 15(c).

## 5. Discussion and Conclusions

### 5.1 Merits of this study

In this study, dynamic illusory motions created by prisms were studied systematically, with the following merits.

(1) In-depth analysis of the eye-movement data:

In this study, three kinds of dynamic motion illusion perception, namely, apparent motion, induced motion, and motion aftereffect, were investigated with the eye-movement data being analyzed from various perspectives including (a) the saccade amplitude of the eyes, (b) the number of fixation times of the eyes, (c) the scan-path distribution of the fixation points, and (d) the difference between two sexes in illusion perceptions.

(2) Acquisition of precise eye-movement data using eye-tracking equipment:

An eye-tracking system is used for acquiring and analyzing precise eye-movement data, avoiding human errors in data measurement. The system consists of an eye-tracking headset and a set of associated equipment including a computer, a display screen, and a turntable with a remote control for rotating objects.

(3) Thorough investigation of various prisms and rotation speeds for illusion creation:

Seven types of prism, including six polygonal and one cylindrical, are tested in the experiments conducted in this study. The required rotation speeds for each prism type to create each of the three types of motion illusion were investigated, facilitating future uses of prism-typed objects for various applications that make use of illusory motions.

- (4) Achieving more effective designs of dynamic geometric forms that satisfy human factors:

The results of the analysis of the motion illusions occurring on the continuous line-graphics on prisms will aid in realizing more effective designs of related dynamic geometric forms that satisfy human factors.

## 5.2 Major research findings of this study

From the facts about the motion illusions derived previously, the following research findings can be identified.

- (1) Polygonal prisms with different numbers of lateral sides, together with the threshold limits of their rotational speeds, affected the formation and properties of the resulting eye-movement data.
- (2) Rotating each prism-type object through a range of speeds from slow to fast creates three types of dynamic motion illusion:

*apparent motion* → *induced motion* → *motion aftereffect*.

- (3) The triangular prism produces the smallest average saccade amplitude for creating the apparent-motion illusion, the largest average saccade amplitude for creating the induced-motion illusion, and again the smallest average saccade amplitude for creating the motion-aftereffect illusion. This trend is roughly also true for the other types of polygonal prism.
- (4) Among the three types of illusory motion, the apparent-motion illusion results in the largest average saccade amplitude.
- (5) The triangular prism is fixated on by the participants roughly for the smallest number of fixation times during the observations of all three types of motion illusion.
- (6) Males and females show no significant difference in their visual reactions to all three types of motion illusion, as proved statistically by independent sample *t*-tests conducted on the saccade amplitudes in the acquired eye-movement data.

## 5.3 Applications of the research results

With the aforementioned merits and findings of this study, the applications of the research results include at least the following aspects.

- (1) Design of dynamic object models or shapes with three-dimensionality on the basis of the apparent-motion illusion:

For example, the average saccade amplitude of the human eyes to observe the apparent-motion illusion created by the rotated triangular prism is the smallest among all the seven types of prism, indicating that staring at such prisms will possibly cause more relaxing and settling effects than other types of prism (i.e., prisms with more than three lateral sides), as discussed previously. As such, triangular prisms may be considered for use in dynamic shape design or object modeling for art exhibitions or illusion shows in small or interior spaces.

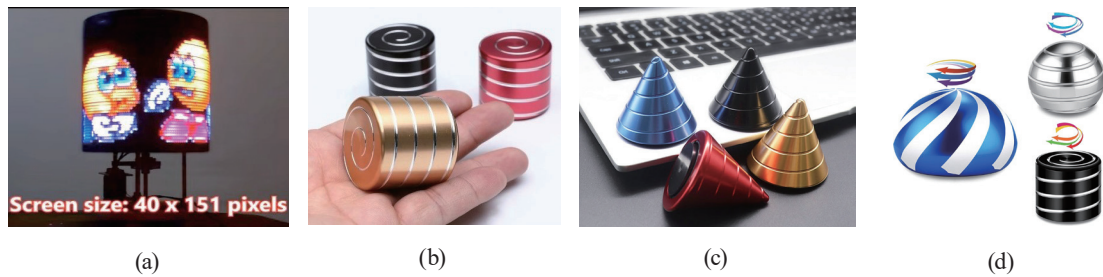


Fig. 16. (Color online) Some existing dynamic objects that create motion illusions. (a) An advertisement sign pillar for use as a signpost based on the POV function to generate the apparent-motion illusion.<sup>(52)</sup> (b)–(d) Desktop toys for decompression while working, based on the induced-motion illusion.<sup>(53–55)</sup>

(2) Design of spinning 3D signs or other types of object on the basis of the induced-motion illusion:

The distribution range of the scan paths for staring at the induced-motion illusion caused by a prism is, in general, large (larger than those of the other two types of motion illusion), as discussed previously. Therefore, prisms may be appropriate for use in designing various kinds of salient dynamical signs or artworks (e.g., advertisement sign pillars, signboards, signposts, toys, artistic cylindrical pillars, etc.) with the induced-motion illusion in larger inner or exterior spaces.

(3) Design of dynamically rotating works on the basis of the motion-aftereffect illusion:

When rotated fast enough, prisms can be observed to yield the dynamic motion-aftereffect illusion and generate afterimages that can be used for designing fascinating fast-rotating works with various types of property (aesthetic, scientific, magical, mysterious, etc.) for displays on various occasions (exhibitions, shows, theme parks, festivals, museums, etc.).

In the future the designing of objects for various applications based on the above ideas may be attempted. Some examples of existing experimental or commercial products that were created by similar ideas are shown in Fig. 16.

#### 5.4 Concluding remarks and suggestions

Different from past studies of motion illusions, eye-tracking equipment was used for the first time in this study to measure accurate eye-movement data from the observation of the illusions for the in-depth analyses of related human reactions. Specifically, the changes in the saccade amplitudes, fixation counts, and scan paths extracted from the eye-movement data were compared, and the correlations or cause-and-effect relationships between these indicators and the three illusory-motion types were analyzed thoroughly. The results indicate that the three types of motion illusion can be generated in order through a range of rotation speeds from slow to fast. Also, polygonal prisms with various numbers of lateral sides were found to affect differently the saccade amplitudes, fixation counts, and scan paths of the eyes during various dynamic illusory-motion perceptions. It is also revealed that no significant difference exists between men and women in their reactions to the three types of dynamic motion illusion created

by various types of prism. Ways in which the research findings can be applied to designs of commonly seen objects with a variety of properties for various activities have also been elaborated.

In the future, the use of dynamic objects other than prisms, such as pyramids and spheres [see Figs. 16(c) and 16(d)], for motion illusion creations can be explored. Furthermore, the answers to other related questions may be sought in further investigations, such as “Are the eye-movement directions and states in various dynamic illusory-motion perceptions all similar?”, “Do scan paths in these illusions have other changes and distribution states?”, “Can illusions other than the three motion-illusion types be incurred using polygonal prisms or pyramids?”. More interestingly, further attempts could be made to apply the findings of these studies to the design of illusion-incurring objects for practical uses in people’s common lives. It is expected that the findings of this study will help advance future studies.

### Acknowledgments

This work was supported in part by the Ministry of Science and Technology, Taiwan under Grant MOST 106-2410-H-224-017-. Special thanks are given to Associate Professor Cheng-Min Tsai of the Department of Visual Communication Design of National Taiwan University of Arts in New Taipei City, Taiwan, for his assistance in the operation of the eye-tracking equipment and in the analysis of statistical data.

### References

- 1 G. D. Chen: Theory and Application of Motion Construction Design (Chuan Hwa Book, Taipei, Taiwan, 2003). <https://www.chuanhwa.com.tw/>
- 2 Wikipedia: Optical illusion. [https://en.wikipedia.org/wiki/Optical\\_illusion](https://en.wikipedia.org/wiki/Optical_illusion) (accessed on 26 March 2023).
- 3 Wikipedia: Illusory motion. [https://en.wikipedia.org/wiki/Illusory\\_motion](https://en.wikipedia.org/wiki/Illusory_motion) (accessed on 25 March 2023).
- 4 E. B. Goldstein: Sensation and Perception (Wadsworth Cengage Learning, Belmont, CA, USA, 2010) 8th ed.
- 5 Wikipedia: Fun with Zoetropes. <https://www.artofplay.com/blogs/stories/fun-with-zoetropes> (accessed on 6 April 2023).
- 6 Wikipedia: Ouchi Apparent Motion Illusion. <https://www.yorku.ca/eye/ouchi.htm> (accessed on 27 March 2023).
- 7 S. E. Palmer: Vision Science (MIT Press, Cambridge, MA, USA, 1999).
- 8 G. D. Chen, C. W. Lin, and H. Fan: J. Science of Design **1** (2017) 47.
- 9 Wikipedia: Barberpole Illusion. [https://en.wikipedia.org/wiki/Barberpole\\_illusion](https://en.wikipedia.org/wiki/Barberpole_illusion) (accessed on 25 March 2023).
- 10 Fotky: Relative Motion Psychology. <https://slk.happyvalentinesday2020.online/relative-motion-psychology-1e67.html> (accessed on 1 September 2023).
- 11 Prairie Creek Makers: Thaumatrope - Early Animation Toy. <https://prairiecreek.typepad.com/makers/2019/03/taumatrope-early-animation-toy.html> (accessed on 5 April 2023).
- 12 Wikipedia: Persistence of Vision. [https://en.wikipedia.org/wiki/Persistence\\_of\\_vision#cite\\_note-Cyclopædia-1](https://en.wikipedia.org/wiki/Persistence_of_vision#cite_note-Cyclopædia-1) (accessed on 5 April 2023).
- 13 G. D. Chen and H. Fan: In Proc. 24th Int. Conf. Human–Computer Interaction (26 June–1 July, 2022) (a virtual conference).
- 14 G. D. Chen, C. W. Lin, and H. Fan: Praxes - Shih Chien University Design Journal **10** (2017) 126.
- 15 C. W. Lin: Study on Motion Perception in Various Forms, Doctorate Dissertation, Graduate School of Design, National Yunlin University of Science and Technology, Chiayi, Taiwan, 2017.
- 16 EyeLink: EyeLink II - Head-Mounted Video-Based Eye Tracker. <https://www.sr-research.com/eyelink-ii/> (accessed on 23 March 2023).

- 17 S. Papavaslopoulou, K. Sharma, and M. N. Giannakos: *Comput. Hum. Behav.* **105** (2020) 1.
- 18 K. Minakata and S. Beier: *Appl. Ergon.* **97** (2021) 1.
- 19 P. Blignaut, E. J. van Rensburg, and M. Oberholzer: *Heliyon* **5** (2019) e01127.
- 20 S. Madariaga, C. Babul, J. Egaña, L. Rubio-Venegas, G. Güney, M. Concha-Miranda, P. E. Maldonado, and C. Devia: *MethodsX* **10** (2023) 102041.
- 21 M. Borys and M. Plechawska-Wójcik: *European J. Medical Technologies* **3** (2017) 11.
- 22 S. Yantis: *Cognitive Psychology* **24** (1992) 295.
- 23 K. Rayner: *Psychological Bulletin* **124** (1998) 372.
- 24 E. H. Hess and J. M. Polt: *Science* **132** (1960) 349.
- 25 J. M. Henderson and A. Hollingworth: *Eye Guidance in Reading and Scene Perception*, G. Underwood, Ed. (Elsevier, Amsterdam, Netherlands, 1998) pp. 269–293.
- 26 K. Gidlöf, A. Wallin, R. Dewhurst, and K. Holmqvist: *J. Eye Movement Research* **6** (2013) 1.
- 27 A. C. Schütz, D. I. Braun, and K. R. Gegenfurtner: *Journal of Vision* **11** (2011) 1.
- 28 Bompas, C. Hedge, and P. Sumner: *Cognitive Psychology* **94** (2017) 26.
- 29 E. D. Megaw and J. Richardson: *Hum. Factors* **21** (1979) 302.
- 30 G. R. Loftus and N. H. Mackworth: *J. Experimental Psychology: Human Perception and Performance* **4** (1978) 565.
- 31 G. T. Buswell: *How People Look at Pictures: A Study of the Psychology of Perception in Art* (Chicago University Press, Chicago, 1935).
- 32 D. Norton and L. Stark: *Sci. Am.* **224** (1971) 34.
- 33 D. Norton and L. Stark: *Science* **171** (1971) 308.
- 34 D. Norton and L. Stark: *Vision Res.* **11** (1971) 929.
- 35 R. W. Backs and L. C. Walrath: *Appl. Ergon.* **23** (1992) 243.
- 36 D. Kahneman and J. Beatty: *Science* **154** (1966) 1583.
- 37 D. Kahneman and P. Wright: *Quarterly J. Experimental Psychology* **23** (1971) 187.
- 38 E. Granholm, R. F. Asarnow, A. J. Sarkin, and K. L. Dykes: *Psychophysiology* **33** (1996) 457.
- 39 G. D. Chen: *The Study of Kinetic Art Dynamic Optical Illusion on Column with Spiral Pattern*, Doctorate Dissertation, Design Institute, National Taiwan University of Science and Technology, Taipei, Taiwan, 2008.
- 40 H. Wallach and K. F. Frey: *Perception and Psychophysics* **11** (1972) 23.
- 41 T. Oyama, S. Imai, and K. Wataru: *New Sensory Perception Psychology Manual* (Seishin Books, Tokyo, 2000).
- 42 M. C. Fu and C. W. Sun: *J. National Taiwan College of Arts* **6** (2010) 125.
- 43 L. Festinger, C. W. White, and M. R. Allyn: *Perception and Psychophysics* **3** (1968) 376.
- 44 S. K. Coren and P. Hoenig: *Perception and Psychophysics* **12** (1972) 224.
- 45 M. C. Fu: *Pursuit Eye Motions on Visual Illusions*, Doctorate Dissertation, Ph.D. Program in Design, Chung Yuan Christian University, Taoyuan, Taiwan, 2009.
- 46 M. C. Fu, C. W. Sun, and P. C. Lin: *Study on Design Science* **13** (2010) 63.
- 47 Q. M. Meng and J. H. Chang: *Experimental Psychology* (Psychological Publishing).
- 48 G. Gescheider: *Psychophysics: The Fundamentals* (Lawrence Erlbaum Associates, Mahwah, NJ, USA, 1997) 3rd ed.
- 49 Wikipedia: Film. <https://en.wikipedia.org/wiki/Film> (accessed 9 April 2023).
- 50 G. D. Chen and C. C. Chang: *Proc. 2007 Conf. Asia Society of Basic Design and Art* (Japan Society of Basic Design and Art, Tsukuba, Ibaraki, Japan, Aug. 2007) 25–27.
- 51 Statistics by Jim: Independent Samples *t* Test: Definition, Using & Interpreting. <https://statisticsbyjim.com/hypothesis-testing/independent-samples-t-test/> (accessed 4 April 2023).
- 52 H. Bauer: *POV Cylinder with Arduino Due*. [https://www.hackster.io/hanoba\\_DIY/pov-cylinder-with-arduino-due-7016d5](https://www.hackster.io/hanoba_DIY/pov-cylinder-with-arduino-due-7016d5) (accessed 5 April 2023).
- 53 GoDream Direct Store: *Desktop Decompression Rotating Cylindrical Gyroscope*. <https://www.aliexpress.com/item/1005001815718386.html> (accessed 5 April 2023).
- 54 Fishpond: *Asuku Kinetic Spinning Desk Toys*. <https://www.amazon.com/asuku-Kinetic-Spinning-Optical-Illusion/dp/B08BKLJ4YX> (accessed 10 April 2023).
- 55 AliExpress: *Rotating Cone Gyroscope Desktop Decompression*. <https://www.aliexpress.com/item/1005004534079896.html> (accessed 10 April 2023).

## About the Authors



**Chih-Chao Chang** received his B.S. degree in 2002 and M.S. degree in 2007, both in visual communication design from Kunshan University of Science and Technology, Tainan, Taiwan. Since 2018, he has been a research assistant in the Interactive Multimedia Design Lab. at the Department of Digital Media Design at National Yunlin University of Science and Technology (YunTech), Yunlin, Taiwan. He is currently a Ph.D. student at YunTech and a member of the Taiwan Society of Basic Design and Art as well as the Color Association of Taiwan. His research interests include digital media design, visual communication, dynamic illusion, eye tracking, light form, and human–computer interaction. ([s650415@yahoo.com.tw](mailto:s650415@yahoo.com.tw))



**Guang-Dah Chen** received his master's degree from Tsukuba National University, Japan, in 1992, and Ph.D. degree from Taiwan University of Science and Technology in 2009. From 1993, he was engaged in design education for many years. From 2001 to 2006, he was the President of the Taiwan Society of Basic Design and Art. Currently, he is an associate professor in the Department of Visual Communication Design at National Taiwan University of the Arts. His current research interests include fundamental design and light art, visual communication, dynamic illusion perception, digital content design, and cross-field integrated design. ([gd196478@yahoo.com.tw](mailto:gd196478@yahoo.com.tw))



**Chao-Ming Wang** received his B.Sc., M.Sc., and Ph.D. degrees in computer science and information engineering from National Chiao Tung University, Hsinchu, Taiwan, in 1980, 1982, and 1993, respectively. From 1982 to 2003, he was a senior specialist at National Chung Shan Institute of Science and Technology. From 2003 to 2008, he was a member of the faculty of the Department of Information Communication at Yuan Ze University, Taoyuan, Taiwan. In 2008, he moved to the Department of Digital Media Design at National Yunlin University of Science and Technology (YunTech). From 2010 to 2013, he was the Head of the Department of Digital Media Design, and from 2016 to 2017, he was the Director of the Design-led Innovation Center, both at YunTech. From 2010 to 2013, he was the President of the Taiwan Society of Basic Design and Art. He is currently a professor in the Department of Digital Media Design at YunTech. His current research interests include computer vision, tech art, human–computer interaction, and interactive multimedia design. ([wangcm@yuntech.edu.tw](mailto:wangcm@yuntech.edu.tw))